



Cite this: *Chem. Commun.*, 2018, 54, 13591

Received 16th October 2018,  
Accepted 2nd November 2018

DOI: 10.1039/c8cc08260j

rsc.li/chemcomm

## Photocontrolled reversible conversion of a lamellar supramolecular assembly based on cucurbiturils and a naphthalenediimide derivative†

Cai-Cai Zhang,<sup>a</sup> Ying-Ming Zhang<sup>a</sup> and Yu Liu<sup>ib</sup> \*<sup>ab</sup>

**Lamellar and helical supramolecular assemblies were constructed using cucurbiturils and a naphthalenediimide derivative. More interestingly, the formation of the lamellar assembly could be reversibly photocontrolled via competitive binding with  $\alpha$ -cyclodextrin and water-soluble azobenzene.**

Supramolecular assemblies constructed using cucurbit[n]urils (CB[n]s) have attracted considerable research interest because of their promising applications in various fields, such as controllable release,<sup>1</sup> drug delivery,<sup>2</sup> luminescent materials,<sup>3</sup> supramolecular catalysts,<sup>4</sup> and chemical sensors.<sup>5</sup> More interestingly, the supramolecular methodology based on CB[n]s as key assembling components provides us with a powerful strategy for the construction of functional nanoassemblies with topological diversity and complexity. For example, Kim *et al.* gave a systematic description of the preparation of hollow nanocapsules through the 'click reaction' between allyloxy-CB[6] and dithiol, exhibiting a promising nanoplatfor for preparing various metal nanoparticles.<sup>6</sup> Scherman *et al.* demonstrated a type of hybrid raspberry-like colloid by employing CB[8]-involved polymeric nanoparticles on silica cores, which showed potential application in organic catalysis and cargo delivery.<sup>7</sup> More impressively, Li, Zhao, and Cao independently reported 2D and 3D supramolecular organic frameworks of CB[8] with pyridinium derivatives.<sup>8</sup> Our group also proposed a supramolecular modulation method mediated by CB[n] to control the topological aggregates of diphenylalanine.<sup>9</sup> These findings definitely showed the potent effect of CB[n] in the morphological interconversion of supramolecular assemblies.

Among the frequently used building blocks, naphthalenediimide (NDI) is a bis-imide derivative of 1,4,5,8-naphthalenetetracarboxylic

dianhydride, which possesses high electron affinity, good charge carrier mobility, and excellent thermal and oxidative stability.<sup>10</sup> The well-defined topological structures based on NDIs have attracted considerable research interest due to their compelling optical and electronic properties. A variety of ingenious nanostructures, including nanorods, vesicles, nanofibers, nanotubes and flower-like structures, have been constructed via chemical modification at the NDI core or on either side of the diimide positions.<sup>11</sup> However, tuning the morphology of NDI-involved nanosystems into well-defined architectures with various dimensions remains a challenging task.

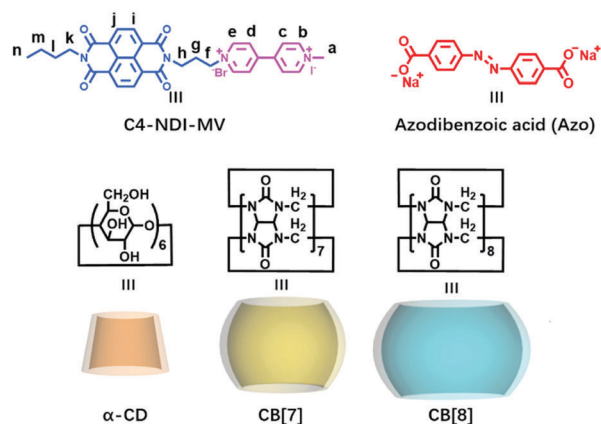
In this work, we wish to report a facile and convenient method to regulate NDI nanostructures via host-guest interactions with CB[7] and CB[8]. In our case, it was found that a supramolecular nanotube was exclusively formed by an amphipathic NDI derivative (C4-NDI-MV). After binding with CB[7] and CB[8], the morphological conversion of C4-NDI-MV occurred from nanotubes to lamellar and helical supramolecular nanoassemblies, respectively. More interestingly, the association and disassociation of the lamellar supramolecular assembly could be reversibly photocontrolled by the photoisomeric complexation between azodibenzoic acid (Azo) and  $\alpha$ -cyclodextrin ( $\alpha$ -CD). A structural illustration of the involved compounds is shown in Scheme 1.

C4-NDI-MV was chosen as the guest molecule because of some of its unique characteristics; (1) the NDI core is available for  $\pi$ - $\pi$  stacking and hydrophobic interactions, thus providing the main driving forces for further assembly; (2) two alkyl chains linked to the NDI core can enhance the hydrophobicity and reinforce the assembly in the aqueous phase; (3) the introduction of a *N*-methyl viologen unit can not only improve the water solubility of C4-NDI-MV but also serve as an anchoring point to bind with different macrocyclic host compounds. Next, the transmission electron microscopy (TEM) images of C4-NDI-MV alone indicated the formation of hollow nanotubes with a uniform diameter of 60 nm (Fig. 1a). The length of the nanotubes was in the range of several hundred nanometres, and it lengthened to more than 2  $\mu$ m over time (Fig. 1b).

<sup>a</sup> College of Chemistry, State Key Laboratory of Elemento-Organic Chemistry, Nankai University, Tianjin 300071, China. E-mail: yuliu@nankai.edu.cn

<sup>b</sup> Collaborative Innovation Center of Chemical Science and Engineering (Tianjin), Tianjin 300072, China

† Electronic supplementary information (ESI) available: Detailed synthesis, characterization data, Job's plots, association constants, absorption spectra and transmission electron microscopy images. See DOI: 10.1039/c8cc08260j



**Scheme 1** Structural illustration of C4-NDI-MV, Azo,  $\alpha$ -CD, CB[7], and CB[8].

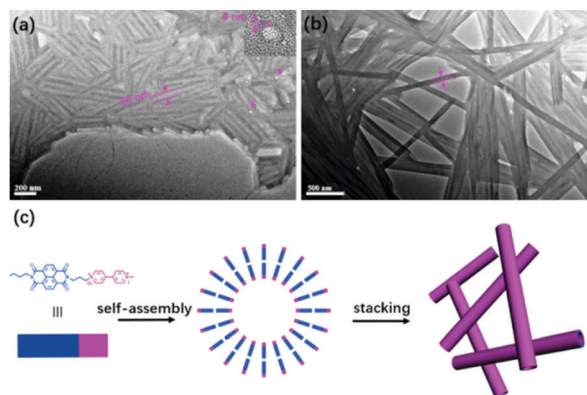


**Fig. 1** (a) TEM image of the self-assembly of C4-NDI-MV (0.03 mM, inset: circular cross section of the nanotubes). (b) TEM image of the self-assembly of C4-NDI-MV stock solution after two days. (c) Proposed self-assembly mode of C4-NDI-MV.

The thickness of the wall was measured from the circular cross section as approximately 6 nm, which was *ca.* two times larger than single C4-NDI-MV (2.8 nm). The internal structure of the C4-NDI-MV nanotubes was subsequently characterized using the X-ray diffraction (XRD) method. As shown in Fig. S15 (ESI<sup>†</sup>), a sharp reflection with a spacing of  $d = 5.6$  nm in the small-angle region was attributed to the length of two fully extended C4-NDI-MV molecules. In addition, the peak at  $d = 3.6$  Å was assigned to the  $\pi$ - $\pi$  stacking distance between the NDI skeleton in the obtained nanotubes. Based on these experimental results, a reasonable model for the nanotubular C4-NDI-MV self-assembly is shown in Fig. 1c. That is, the C4-NDI-MV molecules were arranged in a tail-to-tail manner, and the interior and exterior surfaces of the nanotubes were composed of hydrophilic *N*-methyl viologen units, whereas the hydrophobic NDI cores and alkyl chains were located neatly in the middle interlayer of the tubular walls.

After validating that the exquisite nanotubes could be formed by free C4-NDI-MV, the molecular assembling behaviour was further explored in the presence of CB[7] and CB[8]. First, the binding modes of C4-NDI-MV with CB[7] and CB[8] were investigated using  $^1\text{H}$  NMR experiments. As can be seen

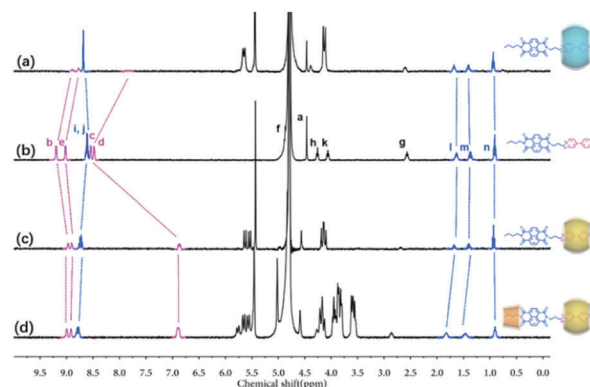


**Fig. 2** Partial  $^1\text{H}$  NMR spectra (400 MHz,  $\text{D}_2\text{O}$ , 25  $^\circ\text{C}$ ) of (a) C4-NDI-MV + CB[8], (b) C4-NDI-MV, (c) C4-NDI-MV + CB[7], and (d) C4-NDI-MV + CB[7] +  $\alpha$ -CD ([C4-NDI-MV] = [CB[7]] = [CB[8]] = [ $\alpha$ -CD] = 1 mM).

from Fig. 2c, the resonance peaks for the protons  $\text{H}_{b-e}$  in the *N*-methyl viologen unit of C4-NDI-MV displayed significant chemical shifts, while those for the NDI core were essentially unchanged, indicating that the *N*-methyl viologen moiety was tightly included in the cavity of CB[7], leaving the NDI moiety outside the cavity.

A similar molecular binding mode was also observed for the inclusion complexation between CB[8] and C4-NDI-MV. That is, the *N*-methyl viologen unit of C4-NDI-MV underwent an obvious up-field shift upon addition of equivalent CB[8] in the  $^1\text{H}$  NMR experiment, once again indicative of the formation of a binary host-guest complex (Fig. 2a). Moreover, Job's plots and mass spectrometric data jointly indicated the 1:1 binding stoichiometry (Fig. S16–S19, ESI<sup>†</sup>), and the association constants ( $K_a$ ) were accordingly calculated as  $3.04 \times 10^5$  and  $4.39 \times 10^5 \text{ M}^{-1}$  with CB[7] and CB[8], respectively, using UV/vis spectroscopy (Fig. S20 and S21, ESI<sup>†</sup>).

Furthermore, the influence of CB[7] and CB[8] on the morphology of C4-NDI-MV was characterized using TEM experiments. As shown in Fig. 3, lamellar nanoassemblies were observed upon complexation of CB[7] with C4-NDI-MV, whereas helical supramolecular assemblies were formed in the case of C4-NDI-MV  $\subset$  CB[8]. The latter phenomenon has been sporadically reported in supramolecular nanosystems, because there is no chiral factor in the C4-NDI-MV or CB[8].<sup>12</sup> Moreover, there was no obvious signal detected in circular dichroism experiments, indicating that no preferential direction was formed in these helical aggregates. The possible mechanism for the macrocycle-induced

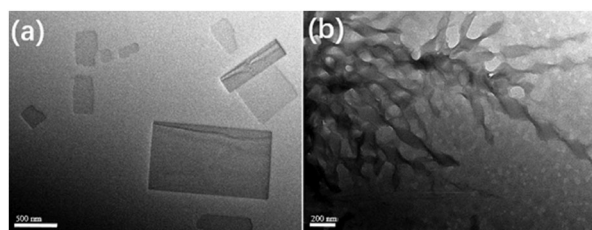
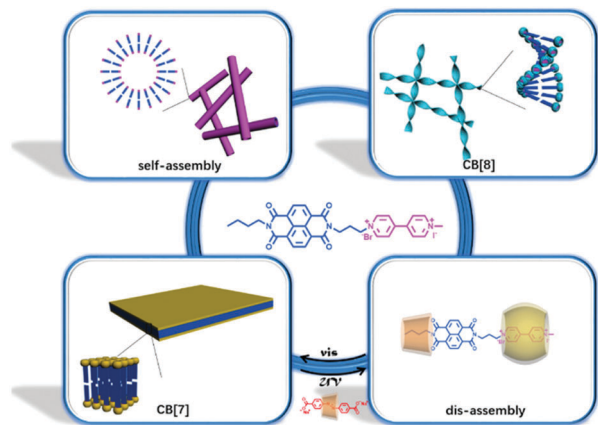


**Fig. 3** TEM images of the (a) C4-NDI-MV  $\subset$  CB[7] and (b) C4-NDI-MV  $\subset$  CB[8] supramolecular assemblies ([C4-NDI-MV] = [CB[7]] = [CB[8]] = 0.03 mM).



**Scheme 2** Proposed supramolecular assembly modes of C4-NDI-MV, C4-NDI-MV  $\subset$  CB[8], C4-NDI-MV  $\subset$  CB[7] and morphological interconversion with Azo  $\subset$   $\alpha$ -CD.

morphological transformation may be explained as follows: the molecular volume of CB[7] is smaller ( $279 \text{ \AA}^3$ ), which means the guest molecules can be neatly accommodated in its cavity, thus resulting in the formation of a lamellar supramolecular assembly. In comparison, the volume of the CB[8] is relatively larger ( $479 \text{ \AA}^3$ ), which is appropriate for the symmetry breaking in the formation of the helical supramolecular assembly.<sup>13</sup> Combining the results described above, we can deduce the assembly process of C4-NDI-MV with CB[7] and CB[8], as shown in Scheme 2.

It is known that alkyl chain moieties can be well encapsulated in the cavity of  $\alpha$ -CD with moderate binding constants.<sup>14</sup> Therefore, in our case,  $\alpha$ -CD was employed to modulate the morphology of the supramolecular assembly. As shown in Fig. 2d,  $^1\text{H}$  NMR experiments were conducted to monitor the intermolecular interaction between C4-NDI-MV  $\subset$  CB[7] and  $\alpha$ -CD. Upon adding  $\alpha$ -CD into C4-NDI-MV  $\subset$  CB[7], the alkyl chain proton signals of C4-NDI-MV exhibited down-field shifts. In comparison, the aromatic proton signals of C4-NDI-MV were almost unchanged. TEM experiments were also performed to investigate the change of the morphology of the lamellar supramolecular assembly of C4-NDI-MV  $\subset$  CB[7] after adding  $\alpha$ -CD (Fig. S22, ESI†). There was no lamellar nanosheet but rather an amorphous morphology in the field of vision, indicating the disassembly of the nanosheets upon addition of excess  $\alpha$ -CD. One reasonable explanation is proposed that the hydrophobic nature of the alkyl chain of C4-NDI-MV is reduced upon immersion into the cavity of  $\alpha$ -CD, thereby resulting in the disassembly of the lamellar C4-NDI-MV  $\subset$  CB[7] aggregation.

Inspired by these promising results and considering the photocontrolled complexation between  $\alpha$ -CD and photoisomeric azobenzenes,<sup>15</sup> we next utilized the carboxylated azobenzene (Azo) as a key component to reversibly switch the lamellar supramolecular architectures of C4-NDI-MV  $\subset$  CB[7]. As shown in Fig. 4g, upon addition of the Azo  $\subset$   $\alpha$ -CD complex into the solution of C4-NDI-MV  $\subset$  CB[7] in  $\text{D}_2\text{O}$ , no obvious chemical shift of the proton signals of the alkyl chain was observed, as a result of more favourable hydrophobic interactions between  $\alpha$ -CD and Azo than with the alkyl chain. After irradiation of the

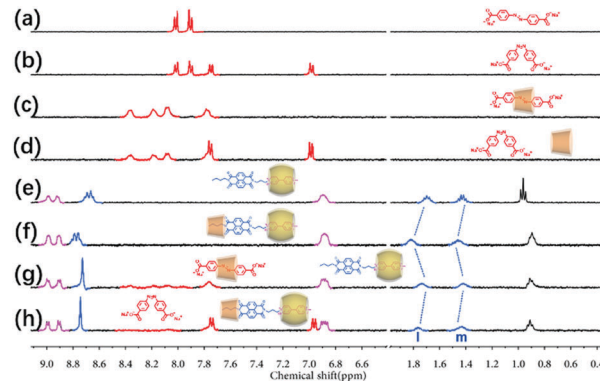


**Fig. 4** Partial  $^1\text{H}$  NMR spectra (400 MHz,  $\text{D}_2\text{O}$ ,  $25^\circ\text{C}$ ) of (a) free Azo, (b) free Azo after UV irradiation, (c) Azo +  $\alpha$ -CD, (d) Azo +  $\alpha$ -CD after UV irradiation, (e) C4-NDI-MV + CB[7], (f) C4-NDI-MV + CB[7] +  $\alpha$ -CD, (g) C4-NDI-MV + CB[7] + Azo +  $\alpha$ -CD, and (h) solution of (e) after UV irradiation ([C4-NDI-MV] = [CB[7]] = [Azo] = [ $\alpha$ -CD] = 1 mM).

four-component solution under UV irradiation at 365 nm, new signals assigned to *cis*-Azo were observed and the alkyl chain protons of C4-NDI-MV exhibited a slight down-field shift (Fig. 4h). These phenomena could be attributed to the photoisomerization of Azo, which could induce the dissociation of the Azo  $\subset$   $\alpha$ -CD inclusion complex. TEM images further corroborated the morphological transformation from the lamellar supramolecular assembly to the amorphous shape in the presence of the Azo  $\subset$   $\alpha$ -CD complex (Fig. 5a and b). Significantly, after the visible light irradiation of the four-component solution at 420 nm, the  $^1\text{H}$  NMR spectra reversed to the original state and the lamellar nanoassemblies reappeared in the TEM images (Fig. 5c).

UV/vis spectroscopy experiments were also performed to explore the reversibility and repeatability of the photocontrolled morphological conversion (Fig. S25, ESI†). As discerned

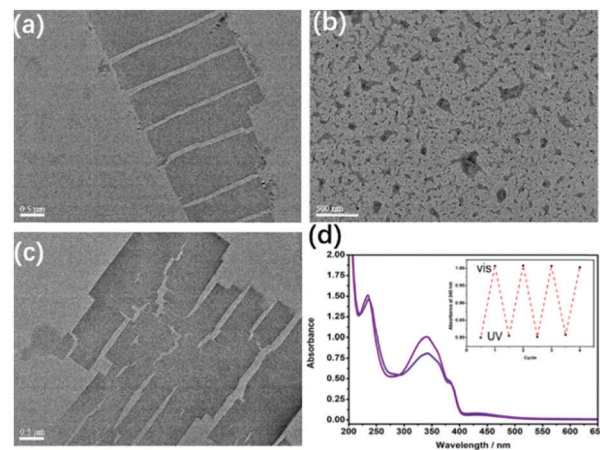


**Fig. 5** TEM image of C4-NDI-MV  $\subset$  CB[7] after adding Azo  $\subset$   $\alpha$ -CD: (a) before light irradiation, (b) after UV irradiation at 365 nm, and (c) after succeeding irradiation with visible light at 420 nm ([C4-NDI-MV] = [CB[7]] = [Azo] = [ $\alpha$ -CD] = 0.03 mM). (d) Cycles of the photocontrolled *trans* and *cis* isomerization of the four-component mixture by alternate irradiation with UV and visible light in the UV/vis spectroscopic experiments ([C4-NDI-MV] = [CB[7]] = [Azo] = [ $\alpha$ -CD] = 0.05 mM), inset: absorbance changes at 340 nm versus cycles.



from Fig. 5d, the reverse isomerization was realized with subsequent irradiation of the four-component solution at 420 nm. It is remarkable that the cycle could be repeated several times without an obvious change in the UV/vis absorption intensity (Fig. 5d, inset). Therefore, it can be concluded that, benefiting from the reversible photoisomerization behavior,  $\text{Azo} \subset \alpha\text{-CD}$  could be utilized as a regulator to efficiently modulate the C4-NDI-MV $\subset$ CB[7] supramolecular architectures with alternating UV/vis irradiation.

In summary, by virtue of the facile host-guest interaction of an amphiphilic NDI derivative with CB[7] and CB[8], we demonstrated a convenient approach to tune the morphology of supramolecular assemblies from hollow nanotubes to lamellar and helical nanostructures. Furthermore, the lamellar nanostructure based on C4-NDI-MV $\subset$ CB[7] complexation could be reversibly photocontrolled upon competitive binding with the  $\text{Azo} \subset \alpha\text{-CD}$  complex. Thus, it can be envisaged that the present study may pave a new way to not only create well-defined nanostructures based on non-covalent interactions but also to attain novel organic electronics and sensors arising from the excellent electrical and optical properties of NDIs.

We thank NNSFC (21432004, 21472100, 21772099, and 91527301) for financial support.

## Conflicts of interest

There are no conflicts to declare.

## Notes and references

- (a) S. Angelos, N. M. Khashab, Y.-W. Yang, A. Trabolsi, H. A. Khatib, J. F. Stoddart and J. I. Zink, *J. Am. Chem. Soc.*, 2009, **131**, 12912–12914; (b) P. Xu, Q. Feng, X. Yang, S. Liu, C. Xu, L. Huang, M. Chen, F. Liang and Y. Cheng, *Bioconjugate Chem.*, 2018, **29**, 2855–2866.
- (a) X.-L. Qiu, Y. Zhou, X.-Y. Jin, Q.-D. Qi and Y.-W. Yang, *J. Mater. Chem. C*, 2015, **3**, 3517–3521; (b) D. Mao, Y. Liang, Y. Liu, X. Zhou, J. Ma, B. Jiang, J. Liu and D. Ma, *Angew. Chem., Int. Ed.*, 2017, **56**, 12614–12618; (c) C. Sun, H. Zhang, S. Li, X. Zhang, Q. Cheng, Y. Ding, L.-H. Wang and R. Wang, *ACS Appl. Mater. Interfaces*, 2018, **10**, 25090–25098.
- (a) X.-L. Ni, S. Chen, Y. Yang and Z. Tao, *J. Am. Chem. Soc.*, 2016, **138**, 6177–6183; (b) Y. Xia, S. Chen and X.-L. Ni, *ACS Appl. Mater. Interfaces*, 2018, **10**, 13048–13052.
- (a) J. A. Finbloom, K. Han, C. C. Slack, A. L. Furst and M. B. Francis, *J. Am. Chem. Soc.*, 2017, **139**, 9691–9697; (b) X. Tang, Z. Huang, H. Chen, Y. Kang, J.-F. Xu and X. Zhang, *Angew. Chem., Int. Ed.*, 2018, **57**, 8545–8549.
- (a) G. Ghale and W. M. Nau, *Acc. Chem. Res.*, 2014, **47**, 2150–2159; (b) W. Zhu, W. Li, C. Wang, J. Cui, H. Yang, Y. Jiang and G. Li, *Chem. Sci.*, 2013, **4**, 3583–3590.
- (a) D. Kim, E. Kim, J. Kim, K. M. Park, K. Baek, M. Jung, Y. H. Ko, W. Sung, H. S. Kim, J. H. Suh, C. G. Park, O. S. Na, D.-K. Lee, K. E. Lee, S. S. Han and K. Kim, *Angew. Chem., Int. Ed.*, 2007, **46**, 3471–3474; (b) G. Yun, Z. Hassan, J. Lee, J. Kim, N.-S. Lee, N. H. Kim, K. Baek, I. Hwang, C. G. Park and K. Kim, *Angew. Chem., Int. Ed.*, 2014, **53**, 6414–6418.
- Y. Lan, Y. Wu, A. Karas and O. A. Scherman, *Angew. Chem., Int. Ed.*, 2014, **53**, 2166–2169.
- (a) K.-D. Zhang, J. Tian, D. Hanifi, Y. Zhang, A. C.-H. Sue, T.-Y. Zhou, L. Zhang, X. Zhao, Y. Liu and Z.-T. Li, *J. Am. Chem. Soc.*, 2013, **135**, 17913–17918; (b) J. Tian, T.-Y. Zhou, S.-C. Zhang, S. Aloni, M. V. Altoe, S.-H. Xie, H. Wang, D.-W. Zhang, X. Zhao, Y. Liu and Z.-T. Li, *Nat. Commun.*, 2014, **5**, 5574; (c) Y. Li, Y. Dong, X. Miao, Y. Ren, B. Zhang, P. Wang, Y. Yu, B. Li, L. Isaacs and L. Cao, *Angew. Chem., Int. Ed.*, 2018, **57**, 729–733.
- W. Zhang, Y.-M. Zhang, S.-H. Li, Y.-L. Cui, J. Yu and Y. Liu, *Angew. Chem., Int. Ed.*, 2016, **55**, 11452–11456.
- (a) Z. Zhao, Z. Yin, H. Chen, L. Zheng, C. Zhu, L. Zhang, S. Tan, H. Wang, Y. Guo, Q. Tang and Y. Liu, *Adv. Mater.*, 2017, **29**, 1602410; (b) T. Kim, R. Younts, W. Lee, S. Lee, K. Gundogdu and B. Kim, *J. Mater. Chem. A*, 2017, **5**, 22170–22179; (c) T. Erdmann, S. Fabiano, B. Milián-Medina, D. Hanifi, Z. Chen, M. Berggren, J. Gierschner, A. Salleo, A. Kiriy, B. Voit and A. Facchetti, *Adv. Mater.*, 2016, **28**, 9169–9174.
- (a) H. Shao, T. Nguyen, N. C. Romano, D. A. Modarelli and J. R. Parquette, *J. Am. Chem. Soc.*, 2009, **131**, 16374–16376; (b) M. B. Avinash and T. Govindaraju, *Nanoscale*, 2011, **3**, 2536–2543; (c) M. B. Avinash, K. Swathi, K. S. Narayan and T. Govindaraju, *ACS Appl. Mater. Interfaces*, 2016, **8**, 8678–8685; (d) M. Al Kobaisi, S. V. Bhosale, K. Latham, A. M. Raynor and S. V. Bhosale, *Chem. Rev.*, 2016, **116**, 11685–11796; (e) M. R. Molla and S. Ghosh, *Chem. Mater.*, 2011, **23**, 95–105; (f) H. Shao and J. R. Parquette, *Chem. Commun.*, 2010, **46**, 4285–4287; (g) M. B. Avinash and T. Govindaraju, *Adv. Funct. Mater.*, 2011, **21**, 3875–3882.
- (a) S. J. George, R. de Bruijn, Ž. Tomović, B. Van Averbek, D. Beljonne, R. Lazzaroni, A. P. H. J. Schenning and E. W. Meijer, *J. Am. Chem. Soc.*, 2012, **134**, 17789–17796; (b) B. Song, Y. Jin, X. He, D. Tang, G. Wu and S. Yin, *Nanoscale*, 2015, **7**, 930–935.
- J. Kim, I.-S. Jung, S.-Y. Kim, E. Lee, J.-K. Kang, S. Sakamoto, K. Yamaguchi and K. Kim, *J. Am. Chem. Soc.*, 2000, **122**, 540–541.
- (a) I. Tomatsu, A. Hashidzume and A. Harada, *Macromolecules*, 2005, **38**, 5223–5227; (b) J. Wang, H.-Y. Zhang, X.-J. Zhang, Z.-H. Song, X.-J. Zhao and Y. Liu, *Chem. Commun.*, 2015, **51**, 7329–7332.
- W. Zhang, Y. Chen, J. Yu, X.-J. Zhang and Y. Liu, *Chem. Commun.*, 2016, **52**, 14274–14277.